

Spectroelectrochemical Investigations of Soluble Polyaniline Synthesized via New Inverse Emulsion Pathway

Subrahmanya Shreepathi and Rudolf Holze*

Institut für Chemie, Technische Universität Chemnitz, AG Elektrochemie, D-09107 Chemnitz, Germany

Received January 19, 2005. Revised Manuscript Received June 1, 2005

A new inverse emulsion protocol has been developed for the synthesis of polyaniline (PANI), which can be dissolved completely in common organic solvents such as chloroform. Benzoyl peroxide is used as the oxidizing agent and toluene + 2-propanol–water is used as the solvent. Dodecylbenzenesulfonic acid (DBSA) has been selected as the dopant because it also functions as the surfactant. Cyclic voltammetry and spectroelectrochemical investigations were carried out to study the electroactivity, UV–Vis response, and metal-to-insulator transition of the chemically synthesized PANI as a function of applied electrode potential. At more positive potentials, cyclic voltammograms of PANI in aqueous acids show two oxidation waves caused by redox processes of PANI as observed with electrochemically prepared PANI. Peak position and shape are influenced by the slow anion exchange rate. Electrical conductivity of the material is relatively high as the minimum resistance value is nearly 10 Ω . SEM investigations show that the amount of DBSA in the feed strongly influences the morphology of the polymer. In situ UV–Vis spectroscopy measurements reveal good electrochromic reversibility for the polymer very similar to the response of PANI synthesized electrochemically.

Introduction

Intrinsically conducting polymers still remain the subject of intense research by many groups worldwide.¹ Continuous attention to polyaniline (PANI) is due to its well-behaved electrochemistry, proton susceptibility, environmental stability, and electrochromism.² Polyaniline is also important in applications such as rechargeable batteries, electromagnetic shielding materials, sensors, electro-optics, and light-emitting diodes.³ It is well-known that polyaniline exists in three different oxidation states; only the polyemeraldine form (leucoemeraldine and pernigraniline are the other two states) is electrically conductive. PANI can be doped electrochemically or chemically with various anions; this results in significant changes in the electronic transport properties of the material.^{4,5} Epstein and co-workers⁶ found that only a fraction of charge carriers in PANI contributed to the observed conductivity (~ 100 S/cm). If all the charge carriers participated in the conduction, PANI should have a conductivity similar to copper. Applications of PANI have been limited by its intractable nature as it is usually obtained chemically as an insoluble powder and electrochemically as a thin brittle film; both are difficult to process.

Considerable progress has been made in the past few years in the processability of polyaniline by synthesis of polymer blends and composites,^{7,8} soluble polyaniline derivatives, and copolymers.^{9,10} However, they have been found to be less conducting than PANI, even though they are more soluble. Meanwhile, several research groups reported enhanced solubility of the parent PANI emeraldine salt when they use bulky acidic groups as a dopant or when they apply a different synthetic route.^{11–17} Laska and Widlarz¹³ have reported synthesis of water-soluble polyaniline with various phosphonic and sulfonic acids as dopants. PANIs in this case are directly produced as dispersions in water and they are stable only for a few days. Kinlen et al.¹⁵ have reported a synthetic protocol for PANI doped with dinonylnaphthalenesulfonic acid (DNNSA). An emulsion polymerization pathway is employed to prepare PANI-DNNSA in the organic phase, which can be purified and extracted as a suspension in organic solvent. However, authors report that reprecipitated PANI has very low solubility. Ito et al.¹¹ have

* To whom correspondence should be addressed. E-mail: rudolf.holze@chemie.tu-chemnitz.de.

- (1) Malinauskas, A. *Polymer* **2001**, *42*, 3957.
- (2) Diaz, A. F.; Bargon, J. In *Handbook of Conducting Polymers*; Skotheim, T. A., Ed.; Marcel Dekker: New York, 1986; Vol. 1, pp 81–116.
- (3) Gustafsson, G.; Cao, Y.; Treac, G. M.; Klavetter, F.; Colaneri, N.; Heeger, A. J. *Nature* **1992**, *357*, 477.
- (4) Kobayashi, T.; Yoneyama, H.; Tamura, H. *J. Electro. Anal. Chem.* **1984**, *161*, 419.
- (5) Chiang, J. C.; MacDiarmid, A. G. *Synth. Met.* **1986**, *13*, 193.
- (6) Kohlman, R. S.; Zibold, A.; Tanner, D. B.; Ihas, G. G.; Inshiguro T.; Min, Y. G.; MacDiarmid, A. G.; Epstein, A. J. *Phys. Rev. Lett.* **1997**, *78*, 3915.
- (7) Anand, J.; Palaniappan, S.; Sathyanarayana, D. N. *Prog. Polym. Sci.* **1998**, *23*, 993.
- (8) Pud, A.; Ogurtsov, N.; Korzhenko, A.; Shapoval, G. *Prog. Polym. Sci.* **2003**, *28*, 1701.
- (9) Zheng, Y. W.; Levon, K.; Laakso, J.; Österholm, J. E. *Macromolecules* **1994**, *27*, 7754.
- (10) Nguyen, M. T.; Kasai, P.; Miller, J.; Diaz, A. F. *Macromolecules* **1994**, *27*, 3625.
- (11) Ito, S.; Murata, K.; Teshima, S.; Aizawa, R.; Asako, Y.; Takahashi, K.; Hoffman, B. M. *Synth. Met.* **1998**, *96*, 161.
- (12) Chen, S. A.; Hwang, G. W. *J. Am. Chem. Soc.* **1995**, *117*, 10055.
- (13) Laska, J.; Widlarz, J. *Synth. Met.* **2003**, *135–136*, 261.
- (14) Palaniappan, S.; Nivasu, V. *New J. Chem.* **2002**, *26*, 1490.
- (15) Kinlen, P. J.; Liu, J.; Ding, Y.; Graham, C. R.; Remsen, E. E. *Macromolecules* **1998**, *31*, 1735.
- (16) Athawale, A. A.; Kulkarni, M. V.; Chabukswar, V. V. *Mater. Chem. Phys.* **2002**, *73*, 106.
- (17) Yin, W.; Ruckenstein, E. *Synth. Met.* **2000**, *108*, 39.

prepared sulfonated polyaniline that can be dissolved up to 88 g/L in water. They adapted a difficult procedure to sulfonate the emeraldine base and the solubility of the resulting material depends on the S/N ratio. However, the conductivity of the PANI is low in the range of 0.02 to 1×10^{-5} S cm⁻¹. Recently, Athawale et al.¹⁶ synthesized polyaniline codoped with acrylic acid but the PANI synthesized is soluble only in NMP and *m*-cresol. Four years ago, Ruckenstein and co-worker¹⁷ reported PANI codoped with HCl and DBSA and the resulting material is soluble in chloroform. Conductivity of PANI prepared is as high as 7.9 S cm⁻¹ but the solubility is not clearly defined. Recently, Sathyanarayana and co-workers^{18,19} successfully used benzoyl peroxide as the oxidizing agent for the polymerization of aniline with many organic and mineral acids as dopants in good yield and conductivity. However, the resulting polymers have low solubility and the authors have not studied PANI doped with DBSA.

In this paper, we report a new inverse emulsion polymerization pathway for the synthesis of PANI doped with DBSA using benzoyl peroxide as the oxidizing agent. DBSA was selected as the dopant because it also functions as a surfactant. DBSA as a large molecule facilitates the solubility of the resulting PANI and benzoyl peroxide has been used for the first time to successfully synthesize PANI-DBSA. The resulting polymer is completely soluble in chloroform and in a 2:1 mixture (v/v) of toluene and 2-propanol. Spectroelectrochemical and cyclic voltammetry investigations of the chemically prepared PANI have been carried out. Influence of the mole ratio of DBSA to aniline on the properties of the PANI is reported.

Experimental Section

Chemicals. Aniline (VEB Laborchemie Apolda, analytical grade) is distilled under reduced pressure and stored under nitrogen. DBSA (70 wt % in 2-propanol, 70% solution, Aldrich) and tetrabutylammoniumtetrafluoroborate (Bu₄NBF₄, Aldrich), fluoroboric acid (as diethyl ether complex purum, Fluka) were used as received. Deionized water (Serapur pro 90 C) was used. All other chemicals were analytical grade reagents and used as procured.

Synthesis of PANI-DBSA. In a typical experiment, 0.303 g of benzoyl peroxide (0.025 M) was added to a 100 mL round-bottomed flask containing 35 mL of toluene. The mixture was kept under mechanical stirring. Ten milliliters of 2-propanol, 1.165 mL of DBSA (0.05 M), and 0.05 mL of aniline (0.01 M) were added to the above mixture. Then 5 mL of water was added to this clear solution to form an inverted emulsion. Here aniline-DBSA salt and 2-propanol in water form the dispersed phase whereas benzoyl peroxide and 2-propanol in toluene form the continuous phase. The reaction mixture gradually turns green in 2.5 h and the stirring was continued for a period of 28 h. In the end, the organic phase containing the polymer was separated and 50 mL of acetone was added to it. PANI phase, which is relatively denser, was then separated from the acetone phase. The separation process was repeated four times and the solvent associated with PANI was evaporated at room temperature for 24 h in a Petri dish. The film

broke into flakes on addition of a small amount of acetone to the Petri dish containing a thick coherent film of PANI. The larger flakes were then separated by hand picking whereas the smaller particles were separated by filtration and the polymer flakes thus obtained were dried in an oven at 50 °C for 4 h.

Polyanilines with different mole ratios of DBSA to aniline (7:1 and 10:1) have been prepared in the same way by keeping the constant oxidant-to-monomer ratio and by varying the concentration of DBSA.

Characterization. UV-Vis spectra were recorded using a Shimadzu 2100 PC spectrophotometer. A quartz cell of 1 cm path length and PANI dissolved in different solvents were used. For the in situ UV-Vis measurements, PANIs dissolved in CHCl₃ are drop coated onto clean ITO-coated glass sheets (indium tin oxide (ITO)-coated glass sheets were supplied by Merck) that were subsequently used as the working electrode. A quartz cell of 1 cm path length fitted with a platinum wire as the counter electrode and saturated calomel electrode (SCE) connected via a salt bridge as a reference electrode served as a three-electrode cell. In situ measurements were carried out under ambient conditions.

Cyclic voltammograms were recorded under a nitrogen atmosphere in a three-electrode H-cell using a custom-built potentiostat connected to a computer with an AD/DA converter. CVs were recorded in three different 1 N aqueous acids (sulfuric, perchloric, and hydrochloric acids) and in a nonaqueous electrolyte solution. For aqueous systems, PANI dissolved in a 2:1 mixture of toluene + 2-propanol and drop-coated onto a glassy carbon electrode (GCE) was used as the working electrode. A Pt sheet and a saturated calomel electrode were used as the counter and reference electrodes, respectively. For nonaqueous systems, PANI dissolved in CHCl₃ and drop-coated onto a Pt sheet was used as the working electrode. Pt sheet electrode and Ag/AgCl in acetonitrile were used as the counter and reference electrodes, respectively. CVs were recorded in acetonitrile containing 0.1 M Bu₄NBF₄ and 0.075 M HBF₄ as the supporting electrolyte.

For in situ conductivity measurements, a double-band gold electrode,²⁰ a gold sheet electrode, and Ag/AgCl in acetonitrile were used as the working, counter, and reference electrodes, respectively. PANI dissolved in chloroform was drop-coated onto a gold double-band electrode and dried at room temperature for 30 min prior to the measurements. A dc voltage of 10 mV was applied to the double-band electrode (gap between the two strips is ~0.05 mm). The current flowing across the band was measured with an I/V converter with an amplification factor (*Fac*) ranging from 10² to 10⁶. The film resistance R_x (ohm) is related to the measured voltage U_x and the amplification factor *Fac* according to

$$R_x = (0.01 \times Fac)/U_x$$

Electrode potential was increased stepwise by 100 mV and after approximately 5 min the electrochemical cell was cut off from the potentiostat. Conductivity measurements were carried out in acetonitrile containing 0.1 M Bu₄NBF₄ and 0.075 M HBF₄ as supporting electrolyte.

In situ pre-resonance Raman spectra were measured on an ISA 64000 spectrometer equipped with a liquid nitrogen cooled CCD camera detector at a resolution of 2 cm⁻¹. Samples were illuminated with 476.5 nm laser light from an argon ion laser Coherent Innova 70. A special three-compartment cell containing 1 N H₂SO₄ was used in the measurements. PANI dissolved in CHCl₃ was drop-coated on a platinum disk electrode polished with γ -Al₂O₃ (0.05 μ m) subsequently used as the working electrode. A platinum sheet

(18) Rao, P. S.; Subrahmanya, S.; Sathyanarayana, D. N. *Synth. Met.* **2002**, *128*, 311.

(19) Rao, P. S.; Palaniappan, S.; Sathyanarayana, D. N. *Macromolecules* **2002**, *35*, 4988.

(20) Holze, R.; Lippe, J. *Synth. Met.* **1990**, *38*, 99; Lippe, J.; Holze, R. *Synth. Met.* **1991**, *41-43*, 2927.

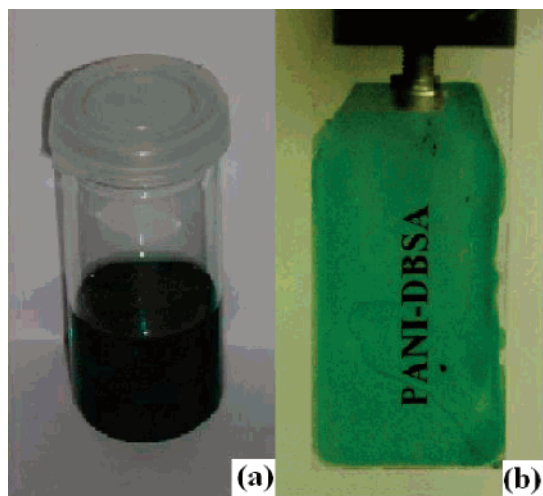


Figure 1. Solution of PANI in a 2:1 mixture of toluene + 2-propanol (a) and its dip-coated film on a glass substrate (b).

electrode and a saturated calomel electrode were used as counter and reference electrodes, respectively. 1 N H₂SO₄ was used as the electrolyte and the cell was purged with nitrogen for 6 min prior to the measurements. The Raman spectra thus obtained were fairly smoothed and baseline-corrected for better visibility. Scanning electron microscope pictures of the solid polymer flakes were recorded using a Philips SEM 515 electron microscope. No gold or platinum coating was applied prior to recording the images. Elemental analysis was carried out using a Vario EL, Elementar Analysensysteme GmbH (Hanau), Elemental Analyzer.

Results and Discussion

Solubility. Solubility of conducting polymers is always a matter of discussion and many reports have been published in the literature discussing the solubility of PANI.^{11,13,16,17} Normally, when a pinch of PANI doped with mineral or organic acid is added to highly polar solvents such as dimethyl sulfoxide (DMSO) or *N*-methylpyrrolidone (NMP), part of the polymer material (presumably oligomeric or of low molecular weight) is dissolved but a residual mass is always present in the mixture. Such a mixture is filtered; by weighing the residual mass, solubility of PANI in g/L is calculated. In this article when we quote “completely soluble” we mean that the PANI is dissolved in the solvent without leaving any solid residue. PANI-DBSA produced in the present way is completely soluble in chloroform and a 2:1 mixture of toluene and 2-propanol. In both solvents it gives a clear green solution (Figure 1a), which can be spin- or drop-coated on metallic and glass substrates. Such films show strong adherence to the substrate. Figure 1b shows a photograph of a dip-coated PANI film on a glass substrate. The transparency of the material is confirmed by the clear visibility of the text (PANI-DBSA), which is nearly 8–10 cm behind the film. Slight solubility is also observed for PANI-DBSA in NMP and in dichloromethane. The PANIs synthesized in the present way are of high purity since the excess of benzoyl peroxide, excess of DBSA, oligomers, and byproducts of oxidation were readily removed by acetone, which was used to wash the organic phase. The polymer samples are labeled as TIP5, TIP6, and TIP7 where the mole ratios of DBSA/aniline in the feed are 5:1, 7:1, and 10:1, respectively.

Table 1. Yield, Conductivity, and Experimental and Calculated Elemental Composition of Polyanilines with Different Mole Ratios of DBSA/Aniline

sample	yield (%)	conductance (1/R Ω ⁻¹)	C, H, N, S analysis	C, H, N, S (calculated)		
				aniline unit	DBSA unit	percentage doping
TIP5	39	0.102	C ₃₄ H ₄₃ N _{2.5} S	(C ₆ H ₆ N) _{2.5}	C ₁₈ H ₂₆ S	40
TIP6	45	0.096	C ₃₃ H ₄₀ N _{2.5} S	(C ₆ H ₆ N) _{2.5}	C ₁₈ H ₂₆ S	40
TIP7	61	0.129	C ₃₃ H ₄₂ N ₂ S	(C ₆ H ₆ N) ₂	C ₁₈ H ₂₆ S	50

Elemental Analysis. The elemental compositions obtained from elemental analysis are in good agreement with the calculated elemental composition (Table 1). N/S ratios obtained from elemental analysis are used to find out the extent of doping (%) and elemental composition of the polymer. Increase in the DBSA/aniline mole ratio from 5:1 to 7:1 does not affect the doping (40% in both the cases) but by changing the mole ratio to 10:1, the doping is increased by 10% (50% doping). Doping in the range of 40–50% always yields very good conductivity for the PANI.

Yield. PANIs synthesized by the present method are obtained in an average yield (Table 1). For the calculation of the yield, we assume 100% doping of the nitrogen atoms in the polymer backbone. The reaction was carried out for a period of 28 h because the yield obtained is optimal after this reaction period. A small amount of polymer is always associated with the acetone, which was used to wash the PANI phase, and therefore reported yields of PANI are average values. Yield increases as the molar ratio of DBSA/aniline in the feed increases. For example, when the ratio of DBSA/aniline is changed from 5:1 to 10:1, the yield increases from 39 to 61%, respectively. This steep increase in the yield may be due to increased pH of the emulsion and higher stability of the emulsion at higher DBSA concentration.

Conductivity. In situ resistance values of all PANIs synthesized by the present method are on the order of 10 Ω (1/R = 0.1, Table 1), which is much higher than the ones reported in the literature.^{21,11,14,15} PANI-DBSA synthesized via gelation method has shown conductivity of the same order of magnitude but the excess of dopant always associated with the polymer reduces the chemical purity of the polymer.²² Conductance of the PANI is proportional to the thickness of the PANI film bridging the two bands but beyond a certain thickness conductivity is not much affected anymore. Higher conductivities in the present case may be due to the bulky dopant DBSA and the preparative method chosen. Figure 2a shows a plot of log *R* vs *E*_{Ag/AgCl} for TIP5 in an anodic and cathodic sweep in the second potential cycle. As the applied potential increases, log *R* remains unchanged until the offset potential for the first oxidation wave in the CV is reached (Figure 2b). Further increase in the potential causes a sharp decrease in log *R* (indicating a sharp increase in conductivity) until the offset of the second oxidation wave in the CV is reached. Resistance increases when the applied potential is further increased. During the cathodic sweep resistance values follow CV and the minimum value of resistance is almost the same as in the case of the anodic

(21) Ahmad, N.; Naseer, J.; Gadgil, N.; Goodson, F. *J. Indian Chem. Soc.* **2004**, *81*, 606.

(22) Madathil, R.; Parkesh, R.; Ponrathnam, S.; Large, M. C. *J. Macromolecules* **2004**, *37*, 2002.

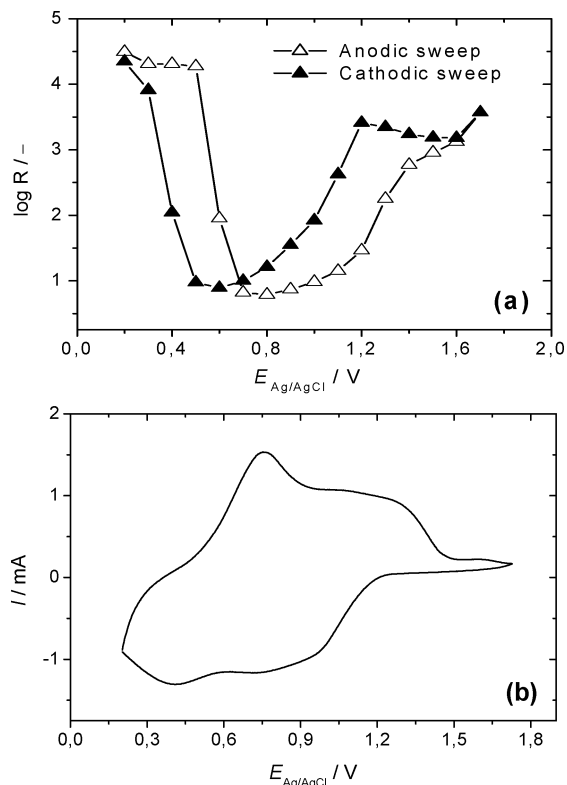


Figure 2. Plot of $\log R$ vs $E_{Ag/AgCl}$ of TIP7 (a) and CV of PANI-modified gold double-band electrode in acetonitrile containing 0.1 M Bu_4NBF_4 and 0.075 M HBF_4 (b).

sweep. This indicates that stability of the PANI bridging the two bands is very good. A similar trend is observed for polyaniline synthesized electrochemically in nonaqueous solvents.²³ However, the minimum resistance during the cathodic sweep is higher than that during the anodic sweep. It is also observed that conductivity of the PANI film was improved after the first potential cycle. This may be due to the conformational changes in the chemically oxidized PANI bridging the two bands induced by the applied potential cycle. The higher potential limit in the conductivity measurements ($E_{Ag/AgCl} = 1.8$ V) slowly damages the film, thereby reducing the conductivity after the second potential cycle. Increase in the mole ratio of DBSA/aniline in the feed does not influence the conductivity of the film. CVs recorded after the conductivity measurements reveal that the conductivity is directly proportional to the anodic peak current. With an increasing amount of PANI bridging the two bands, the anodic peak response in CV is higher and thus measured conductivity is higher.

Our attempt to measure the resistance values of the PANI in aqueous acids failed; the $\log R$ values were in the range of 5 and 6 for all applied potentials. Such different behavior of conductivity in aqueous and nonaqueous electrolyte solutions is due to the presence of the long chain bulky dopant. This influence was later confirmed by cyclic voltammetry studies. Polar groups of this dopant are engaged in protonation of the nitrogen atoms whereas the nonpolar aliphatic chain is extended to the environment leading to a repulsive interaction with aqueous electrolyte solution.

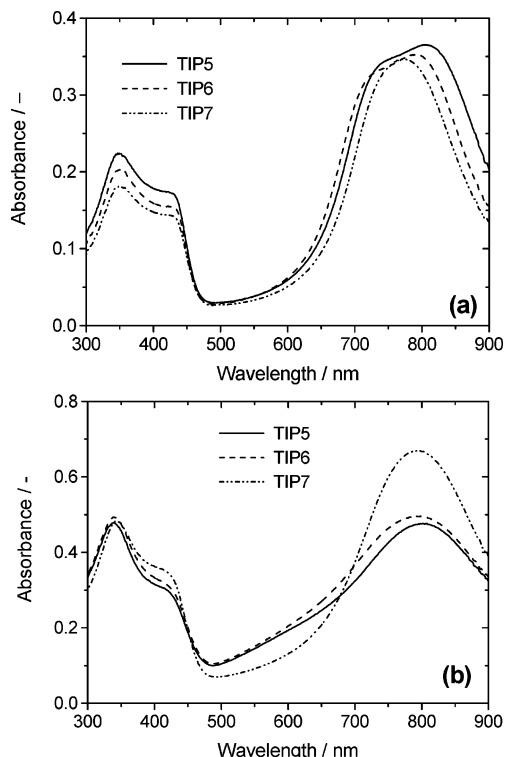


Figure 3. Electronic absorption spectra of PANI with different feed ratios of DBSA/aniline recorded in (a) $CHCl_3$ and (b) 2:1 toluene + 2-propanol.

UV–Vis Spectroscopy. Figure 3a,b shows absorption spectra of polyaniline with different molar ratios of DBSA to aniline in chloroform and in a 2:1 mixture of toluene and 2-propanol. Polyaniline dissolved in chloroform or in a toluene + 2-propanol mixture (2:1) shows three bands characteristic of the emeraldine salt. A band at 350 nm arises from the $\pi \rightarrow \pi^*$ transition while the bands at 420 and 800 nm originate from the charged cationic species known as polarons.¹⁷ In addition, a hump at around 735 nm is observed for TIP5 and TIP6 in chloroform with unknown cause. PANI dissolved in chloroform shows a hypsochromic shift when the mole ratio of DBSA in the feed is increased from 5:1 to 10:1 (Figure 3a). Such blue shift was observed by Yin and Ruckenstein¹⁷ for PANIs codoped with HCl and DBSA. They suggested that an increase in the amount of HCl in the polymer increases the compact coil conformation of the polymer, leading to a hypsochromic shift. Increase in the dopant ions favors the compact coil conformation and thus the absorption maximum is shifted to lower wavelengths. Such hypsochromic shift is not observed for PANI dissolved in a 2:1 mixture of toluene and 2-propanol (Figure 3b). However, interestingly the ratio of intensity of the band at 800 nm to the band at 350 nm is much higher for TIP7, indicating a higher concentration of polaronic species generated from higher doping (Table 1).

Figure 4 shows in situ UV–Vis spectra recorded in 1 N H_2SO_4 at different potentials successively shifted into the anodic direction for TIP7. An absorption band at 800 nm shows a blue shift as the applied potential increases from $E_{SCE} = -0.2$ to 0.8 V. The gradual blue shift of this band is attributed to the formation of a compact coil structure due to the incorporation of SO_4^{2-} ions. When the potential passes $E_{SCE} = 0.6$ V, a drastic blue shift is observed, which

(23) Vogel, S.; Holze, R., *Electrochim. Acta*, **2005**, *50*, 1587.

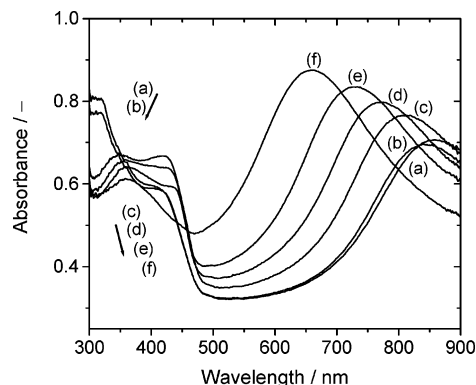


Figure 4. In situ electronic absorption spectra of PANI (TIP7) recorded in ongoing anodic potential direction in 1 N H₂SO₄. E_{SCE} = (a) -0.2, (b) 0, (c) 0.2, (d) 0.4, (e) 0.6, and (f) 0.8 V.

corresponds to the conversion from the emeraldine state to the pernigraniline state. Dominis et al.²⁴ observed that the absorption maximum of redoped PANI in two different solvents is different. They have attributed this difference to the compact and extended coil conformation of the PANI where the compact coil form shows absorption maxima at higher energies. Absorbance at 420 nm originates from radical cations, showing a maximum value at $E_{SCE} = 0.2$ V, indicating a maximum concentration. At $E_{SCE} = 0.2$ V the first oxidation wave peaks in the CV have maximum peak current (Figure 6a). In situ spectral investigations reveal that polarons exist even at $E_{SCE} = -0.2$ V (identified with their 420 nm band) where PANI exists in the completely reduced leucoemeraldine state. Similar trends have been observed for PANI-H₂SO₄ synthesized electrochemically on an indium tin oxide-coated glass electrode.²⁵ However, the latter authors do not give any explanation for the shifts they have observed. The position of the band at 350 nm is influenced by the extent of conjugation in the polymer backbone. Increasing the applied potential from $E_{SCE} = -0.2$ to $E_{SCE} = 0.8$ V, this band shifts toward lower energy and the absorbance of this band is decreased.

In situ electronic absorption spectra were also recorded in the cathodic direction to check the electrochromic reversibility of the polymer film. Figure 5 shows plots of λ_{max} and absorbance at λ_{max} vs applied potential. It is clear from the figure that PANI films have very good electrochromic reversibility. λ_{max} at 800 nm shows linear dependency with applied potential. This linear dependency improves as the molar ratio of DBSA/aniline in the feed is increased. It is also observed that increase in the concentration of DBSA in the feed improves the reversibility of the absorbance at λ_{max} . In the potential range of $E_{SCE} = 0.1$ – 0.9 V, PANI films exist in emeraldine and pernigraniline oxidation states. There exists an isosbestic point at 460 nm in this potential range, indicating a one-step transition from the emeraldine to the pernigraniline state (Figure 4).²⁶ Recently, MacDiarmid and co-workers²⁷ carried out a detailed study with UV-Vis

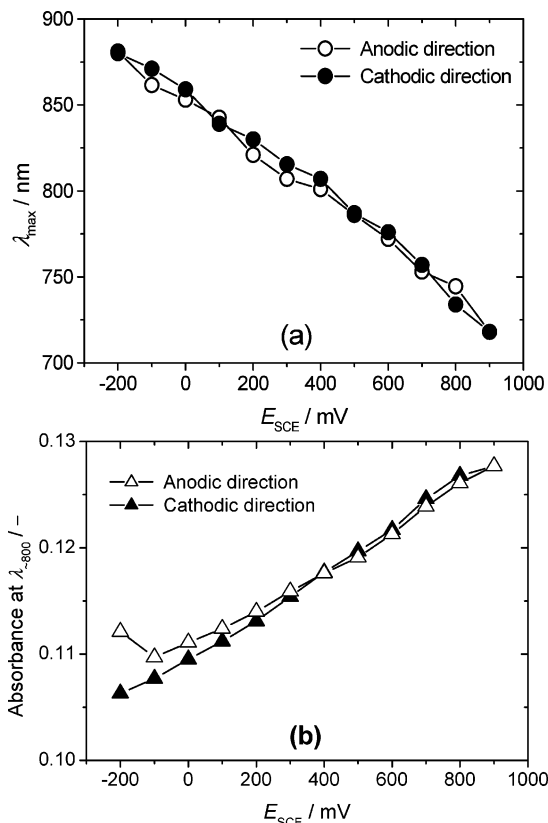


Figure 5. Plots of λ_{max} (a) and absorbance at λ_{max} (b) versus applied potential for PANI (TIP7).

spectroscopy during interconversion of different oxidation states of the PANI, where they have observed two isosbestic points, which they attributed to the interconversion of all three oxidation states.

Cyclic Voltammetry. Representative CVs of TIP5 in three different aqueous mineral acids are shown in Figure 6a. There are two pairs of redox peaks almost similar to the ones observed with PANI prepared electrochemically in aqueous acids. A first oxidation wave around $E_{SCE} = 0.2$ V is assigned to the leucoemeraldine to emeraldine transition and the second oxidation wave at around $E_{SCE} = 0.8$ V is due to the transition from the emeraldine to the pernigraniline state. During the first 20 cycles, the second oxidation wave shifts to more negative potentials and a dramatic decrease in the peak current is observed. A new oxidation wave starts to appear at $E_{SCE} = 0.5$ V and its current density gradually increases. In the case of HCl, the new band grows much faster than those with the other two acids. This is attributed to a kinetic effect, i.e., slow exchange of the anions in the acid and the bulky dopant anions present in the polymer film. Thus, the two oxidation waves in the region of $E_{SCE} = 0.5$ – 0.8 V may originate from two different counterions in the system. Dominis et al.²⁴ observed that PANI redoped with DBSA does not show distinct redox waves. They quote that the surfactant-like nature of the dopant hinders the charge transfer due to poor wettability of the polymer by the aqueous electrolyte. A hump observed in the region of 0.3–0.5 V arises from products of overoxidation.²⁸ The cathodic part of the CV exhibits complicated features; the waves are broad

(24) Dominis, A. J.; Spinks, G. M.; Kane-Maguire, L. A. P.; Wallace, G. *Synth. Met.* **2002**, *129*, 165.

(25) Li, C.; Mu, S. *Synth. Met.* **2004**, *144*, 143.

(26) Lindfors, T.; Kvarnström, C.; Ivaska, A. *J. Electroanal. Chem.* **2002**, *518*, 131.

(27) de Albuquerque, J. E.; Mattoso, L. H. C.; Faria, R. M.; Masters, J. G.; MacDiarmid, A. G. *Synth. Met.* **2004**, *146*, 1.

(28) Abd-Elwahed, A.; Holze, R. *Synth. Met.* **2002**, *131*, 61.

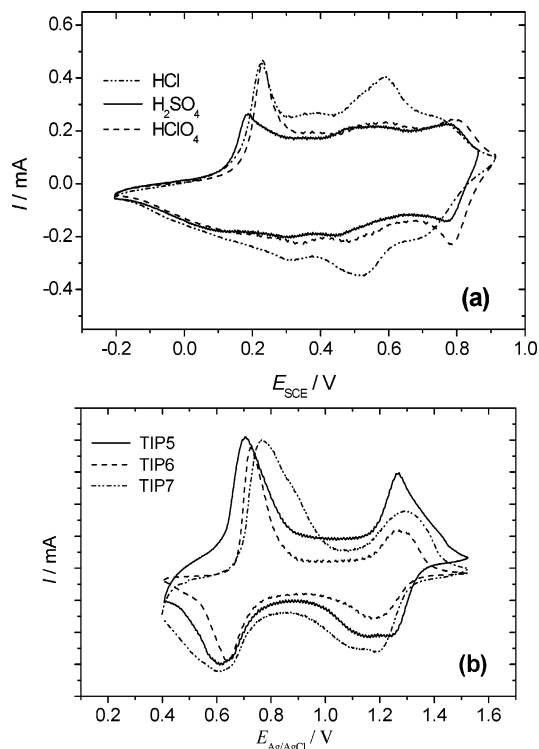


Figure 6. CVs of (a) TIP5-coated GCE electrodes in three different acids at a scan rate of 50 mV/s and (b) PANIs with different mole ratios of DBSA/aniline-coated on a platinum sheet electrode at a scan rate of 50 mV/s recorded in acetonitrile containing 0.1 M Bu₄NBF₄ and 0.075 M HBF₄.

and overlapping.²⁹ It is also observed that anodic peak currents are relatively higher than the cathodic ones. Jiang and Dong³⁰ have observed the same behavior for soluble polyaniline synthesized by the treatment of emeraldine base with boiling 2 M NaOH. They conclude that the rate of proton elimination in the anodic process is greater than that of the proton addition reaction in the cathodic process, leading to higher and sharper peak currents in the anodic process.

Cyclic voltammograms of PANI in acetonitrile containing 0.1 M Bu₄NBF₄ + 0.075 M HBF₄ with different molar ratios of DBSA/aniline in the feed are shown in Figure 6b. CVs show two pairs of well-defined redox waves similar to the ones synthesized electrochemically in aqueous acids.²⁹ Electroactivity of the PANI in nonaqueous solvents is very good when compared to those of aqueous electrolytes, even though they have low pH. As mentioned earlier, this difference arises from the poor wettability of the PANI film in aqueous media. CVs are reproducible for several cycles, indicating the absence of any free monomers or oligomers in the PANI. When cycled up to $E_{Ag/AgCl} = 2.0$ V overoxidation takes place, which is reflected by a gradual decrease in the peak current. An increase in the amount of DBSA in the feed shifts the position of the first oxidation wave to more positive potentials (Figure 6b). As mentioned earlier, an increasing amount of dopant in the polymer leads to the formation of compact coil structures, thereby shifting the position of the oxidation wave to more positive potentials. Figure 7 shows

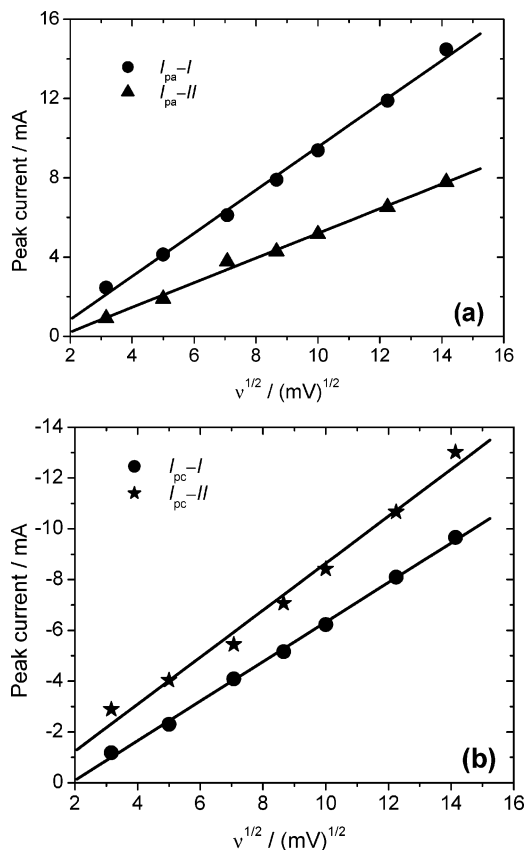


Figure 7. Plots of anodic (I_{pa}) [a] and cathodic (I_{pc}) [b] peak currents versus square root of the scan rate [$(\nu)^{1/2}$].

plots of anodic and cathodic peak currents vs square root of the scan rate. The plots yield straight lines, indicating that the electrochemical processes are diffusion-controlled.³⁰ Normally in ideal diffusion-controlled systems, the intercept of the plot is zero, but in the case of conducting polymers contributions such as double-layer charging disturb the concept of zero intercept. Plots of current/square root of the scan rate vs $E_{Ag/AgCl}$ (not shown here) yield identical values of current/square root of scan rate at the peak maxima, confirming the diffusion-controlled process. The straight lines in Figure 7 also indicate that electrochemical behavior of PANI synthesized by our method is similar to that electrochemically synthesized.

In Situ Pre-resonance Raman Spectroscopy. Pre-resonance enhancement^{31,32} for the PANI films was effective because the laser excitation wavelength used ($\lambda_0 = 476.5$ nm) matches the higher wavelength wing of the absorption band of the PANI centered at 420–430 nm. In situ UV–Vis spectra reveal that, during an anodic potential sweep, absorbance of the band at 430 nm increases, passes through a maximum, and then decreases as shown in the inset of Figure 8. Frequencies of the major bands and their assignments are summarized in Table 2. At $E_{SCE} = -0.2$ V the Raman spectrum shows two strong peaks at 1628 and 1194 cm^{-1} assigned to benzoid ring modes (Table 2). The intensity of almost all the peaks increases when the applied potential

(29) Lapkowski, M.; Berrada, K.; Quillard, S.; Louran, G.; Lefrant, S.; Pron, A. *Macromolecules* **1995**, *28*, 1233.

(30) Jiang, R.; Dong, S. *Synth. Met.* **1988**, *24*, 255.

(31) Gardiner, D. J.; Graves, P. R., Eds. In *Practical Raman Spectroscopy*; Springer-Verlag: Berlin, 1989; p 9.

(32) Andrews, D. L. In *Lasers in Chemistry*; Springer-Verlag: Berlin, 1986; p 106.

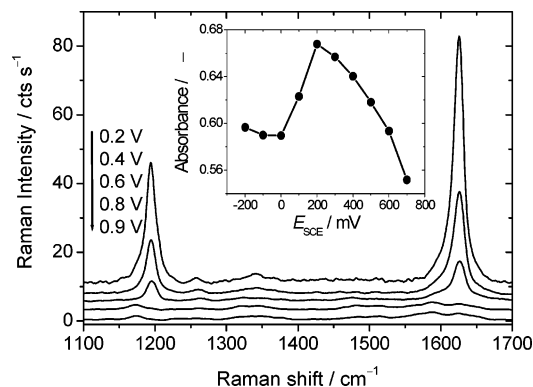


Figure 8. In situ pre-resonance Raman spectra of PANI (TIP7) recorded in 1 N H₂SO₄ using $\lambda_0 = 476.5$ nm laser excitation at various applied electrode potentials. Inset: Plot of the absorbance at 430 nm against the applied potential obtained from in situ electronic absorption spectra.

Table 2. Major Raman Bands and Their Assignments for a PANI Film Recorded in 1 N H₂SO₄, $\lambda_0 = 476.5$ nm

frequency (cm ⁻¹)	state ^a	assignment ³⁴
1626–1630	B	C–C ring stretching
1585–1600	Q	C–C ring stretching
1506–1516	Q	Cd=N stretching
1480–1486	Q	Cd=N stretching
1339–1349	SQR	C–N ⁺ stretching
1257–1266	B	C–N stretching
1190–1197	B	C–H in-plane bending
1171–1174	Q	C–H in-plane bending
885	B	in-plane ring deformation
830–836	Q	in-plane ring deformation
800–815	Q	C–H out-of-plane bending
712–724	B	out-of-plane ring deformation
685–698	Q	out-of-plane ring deformation
636	B	in-plane ring deformation
511–526		out-of-plane C–N–C torsion
412–420	Q	out-of-plane C–H wag

^a B = benzoid ring, Q = quinoid ring, and SQR = semiquinone radical.

is raised to $E_{SCE} = 0.2$ V; beyond this value scattered light intensity decreases with further positive going electrode potential. This trend of potential-dependent pre-resonance enhancement is very similar to the plot of absorbance at 430 nm vs applied potential (inset of Figure 8).

Particularly, intensity of the 1628 and 1194 cm⁻¹ bands bleaches almost by 2 orders of magnitude at higher positive potentials (Figure 8).³³ During an anodic sweep, a new band appears in the range of 680–690 cm⁻¹ at $E_{SCE} = 0.1$ V and disappears at $E_{SCE} = 0.6$ V. Liu et al.³⁴ assign this band to an out of plane ring deformation of the quinoid ring. As the band exists only in the potential region of the emeraldine state of PANI, this band may be caused by the semiquinone radical and not the quinoid ring. Two bands at 980 and 1005 cm⁻¹ of weak to medium intensity are caused by internal modes of the sulfate anion; the band at 980 cm⁻¹ is present at all applied potentials.³³ A band in the range of 1040–1057 cm⁻¹, which is present at all applied potentials, and a band at 1120 cm⁻¹ originate from the dopant, DBSA. These bands are assigned to C–S stretching and S=O out-of-plane bending modes, respectively.³⁵

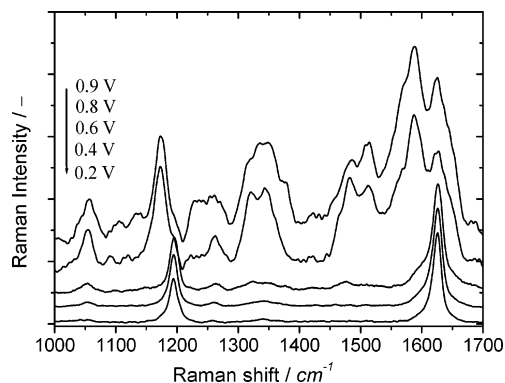


Figure 9. In situ pre-resonance Raman spectra of PANI (TIP7) recorded in 1 N H₂SO₄ using $\lambda_0 = 476.5$ nm laser excitation at various applied electrode potentials (stacked for better visibility).

A band at 1345 cm⁻¹ is assigned to the C–N stretching vibration of the semiquinone radical state (Table 2); this band exists even at $E_{SCE} = -0.2$ V, indicating that some radical cations are still present in the leucoemeraldine state, which is also confirmed by in situ UV–Vis spectroscopy. At higher positive potentials, a new band at 1327 cm⁻¹ appears and the intensity of this band increases, whereas the intensity of the band at 1345 cm⁻¹ decreases as the potential is increased in the positive direction. New bands start to appear in the region of 1480–1520 cm⁻¹ at or after $E_{SCE} = 0.6$ V. When the applied potential is more than $E_{SCE} = 0.6$ V, PANI exists mainly in the pernigraniline state where the polymer backbone has more quinoid ring units. Figure 9 shows in situ pre-resonance Raman spectra of PANI at different applied potentials. The new bands in the region of 1480–1520 cm⁻¹ and at 1590 cm⁻¹ are caused by modes of the quinoid structure. However, the band at 1590 cm⁻¹ shows a red shift when the applied potential is increased from $E_{SCE} = 0.6$ to $E_{SCE} = 0.8$ V. Goff and Bernard³⁶ stated that there should be three C–C ring stretching modes (1550, 1575, and 1585 cm⁻¹) and two C=N stretching modes (1485 and 1500–1515 cm⁻¹) for quinoid rings. They have also observed that C–C ring stretching modes are sensitive to the applied potential and pH of the medium whereas the multiplicity in C=N stretching arises from the difference in protonation and charge localization on the imine sites. The low-frequency shift we observed may be due to the weakening of C=N bond strength at higher potential where the next step is overoxidation. The new bands assigned to quinoid ring at higher potential clearly indicate the transformation from the conducting emeraldine state to the nonconducting pernigraniline state and thus in situ Raman spectroscopy can be used to monitor the conductor to insulator transition.

Scanning Electron Microscopy. Morphological investigations were carried out using scanning electron microscopy (SEM) to study the influence of the amount of DBSA in the feed on morphology. It is well-known that morphology of PANI is influenced by the method of synthesis and the oxidizing agent employed.³⁷ SEM micrographs recorded at lower resolution for all the samples show porous film and smooth film morphology for the surface open to the

(33) Sariciftci, N. S.; Kuzmany, H. *Synth. Met.* **1987**, *21*, 157.

(34) Liu, C.; Zhang, J.; Shi, G.; Chen, F. *J. Appl. Polym. Sci.* **2004**, *92*, 171.

(35) Xu, C. Y.; Zhang, P. X.; Yan, L. *J. Raman Spectrosc.* **2001**, *32*, 862.

(36) Goff, A. H.-L.; Bernard, M. C. *Synth. Met.* **1993**, *60*, 115.

(37) Rao, P. S.; Subrahmanya, S.; Sathyanarayana, D. N. *Synth. Met.* **2003**, *139*, 397.

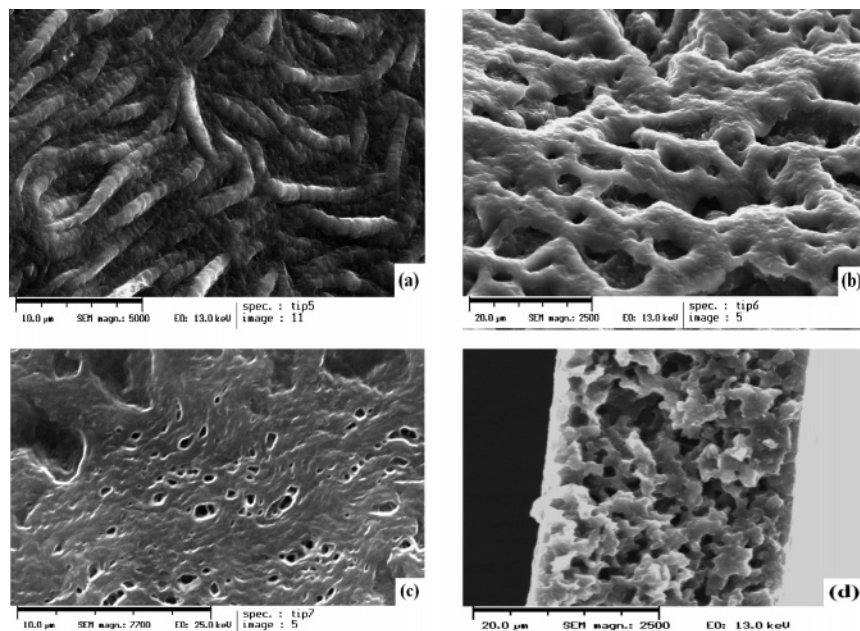


Figure 10. SEM micrographs of PANI-DBSA at (a) 5:1, (b) 7:1, and (c) 10:1 feed ratios of DBSA to aniline. (d) Cross-sectional view of image (b).

environment and the surface in contact with glass substrate during evaporation of the solvent, respectively. The size of the pores varies from 20 to 150 μm and they arise when evaporation of the solvent is carried out during synthesis. SEM pictures reveal that PANI flakes are formed during layer-by-layer stacking of the polymer. High-resolution SEM micrographs reveal that morphology of PANI is strongly influenced by the mole ratio of DBSA/ aniline in the feed. Figure 10 shows SEM images of PANI-DBSA flakes at different molar ratios of DBSA/ aniline in the feed. TIP5 (DBSA/aniline is 5:1) exhibits fibrillar morphology (Figure 10a) where the fibers are approximately 8 μm in length and 1 μm in width. When the ratio of DBSA to aniline is increased to 7:1 (TIP6) and 10:1 (TIP7), morphology changes to porous network type (Figure 10b) and compact film type (Figure 10c), respectively. A cross-sectional view shows a porous network type of morphology (Figure 10d). SEM images of PANI-DBSA synthesized via gelation also exhibit a stacked layer-by-layer morphology and the surface of the gel exhibits fibrillar morphology.²² The change in the morphology due to the change in the mole ratio of DBSA to aniline may be caused by a change in conformation of the polymer. At higher DBSA to aniline mole ratios, PANI prefers compact film morphology.

Conclusions

A new inverse emulsion procedure is successfully employed to synthesize PANI-DBSA, which is completely soluble in common organic solvents such as chloroform and a 2:1 mixture of toluene and 2-propanol. PANI redissolved in these solvents can be spin-, drop-, or dip-coated on metallic or glass substrates with very good adhesion. PANI suspension obtained during synthesis can also be used directly for practical applications. The polyanilines prepared have very good electrochromic reversibility and good conductivity. Cyclic voltammetry studies reveal that electroactivity of PANI is much better in nonaqueous electrolytes than in aqueous electrolytes and the CVs of PANI are almost similar to the ones synthesized electrochemically. In situ pre-resonance Raman spectroscopy is used to monitor metal to insulator transition in PANI. The amount of DBSA in the feed strongly influences the morphology of the polymer but the other properties of the polymer such as conductivity and solubility are not much affected.

Acknowledgment. Financial support by the Deutsche Forschungsgemeinschaft (GRK 829/1) is gratefully acknowledged. We thank Mrs. Baumann, Institute of Physics, TU Chemnitz, for help in recording SEM micrographs.

CM050117S